Journal of Power Sources 196 (2011) 6029–6035

Contents lists available at ScienceDirect

Journal of Power Sources

journal homepage: www.elsevier.com/locate/jpowsour

# Biofilm formation and electricity generation of a microbial fuel cell started up under different external resistances

Liang Zhang[a,b], Xun Zhu[a,b,*], Jun Li[a,b], Qiang Liao[a,b], Dingding Ye[a,b]

[a] Key Laboratory of Low-grade Energy Utilization Technologies and Systems, Chongqing University, Chongqing 400030, China
[b] Institute of Engineering Thermophysics, Chongqing University, Chongqing 400030, China

ARTICLE INFO

*Article history:*
Received 9 February 2011
Received in revised form 4 April 2011
Accepted 5 April 2011
Available online 12 April 2011

*Keywords:*
External resistance
Microbial fuel cell
Power density
Sustainable current generation
Biofilm structure

ABSTRACT

To investigate the effects of external resistance on the biofilm formation and electricity generation of microbial fuel cells (MFCs), active biomass, the content of extracellular polymeric substances (EPS) and the morphology and structure of the biofilms developed at 10, 50, 250 and 1000 Ω are characterized. It is demonstrated that the structure of biofilm plays a crucial role in the maximum power density and sustainable current generation of MFCs. The results show that the maximum power density of the MFCs increases from $0.93 \pm 0.02\ W\ m^{-2}$ to $2.61 \pm 0.18\ W\ m^{-2}$ when the external resistance decreases from 1000 to 50 Ω. However, on further decreasing the external resistance to 10 Ω, the maximum power density decreased to $1.25 \pm 0.01\ W\ m^{-2}$ because of a less active biomass and higher EPS content in the biofilm. Additionally, the 10 Ω MFC shows a highest maximum sustainable current of $8.49 \pm 0.19\ A\ m^{-2}$. This result can be attributed to the existence of void spaces beneficial for proton and buffer transport within the anode biofilm, which maintains a suitable microenvironment for electrochemically active microorganisms.


## 1. Introduction

Microbial fuel cell (MFC) is an economical pathway to a sustainable energy future. In a typical MFC, electron donors, such as organic materials in waster, are oxidized by the electrochemically active bacteria mostly growing as a biofilm on the anode surface [1,2]. Although experiencing a significant development in recently years, the power generation is still insufficient for the practical applications. In order to improve the MFC performance, efforts have been made to enrich more electrochemically active bacteria [3–5], to improve reactor configuration [6–10], to identify better electrode materials [6,8–12], as well as to optimize process parameters [6,13].

Optimizing the growth conditions for the electrochemically active bacteria in the anode was also an important consideration for improving the performance of MFCs. Many factors, such as nutrient supply, flow rate, pH, temperature [2,6,7,14,15], have been found to strongly affect the MFC performance and start-up time. One of the most important and most investigated factors is the anode potential at which the MFC is operated, as it controls the theoretical energy gain for microorganisms [16]. Finkelstein et al. [17] reported that a larger and earlier maximum current were obtained at a more positive applied potential due to the increased energy yield for microbial colonization. In addition, Aelterman et al. [4] found that the anode potential had no influence on the start-up time but an improved current and power generation can be obtained at an optimal anode potential of −200 mV vs. Ag/AgCl. Wang et al. [18] reported that a poised potential of 200 mV (vs. Ag/AgCl) accelerated the start-up of MFCs. Recently, Wei et al. [19] investigated the current and biomass production of *G. sulfurreducens* growing on anodes at a potential of −160, 0, and 400 mV (vs. SHE). The results indicated that faster start-up times, higher current generation and greater biomass production were achieved when the anode set to 0 and 400 mV.

Besides the anode potential, the effect of external resistance applied to the electrical circuit also received wild attention since controlling the growth condition for the electrochemically active bacteria by changing the external resistance is more feasible than poising the anode potential in MFC applications. Generally speaking, MFC performance increases with decreasing the applied external resistance. Liu et al. [20] demonstrated that the lower external resistance was applied, the higher maximum power output was obtained. Aelterman et al. [12] reported a significant increase both in continuous current generation and in power generation when the external resistance of MFCs was lowered from 50 to 25 and then to 10.5 Ω when the MFC was operated at each resistance for 9–11 days. In addition, the changes in the microbial diversity and metabolism were also noted when different external resistances were applied to the MFCs. Lyon et al. [21] observed

* Corresponding author at: Key Laboratory of Low-grade Energy Utilization Technologies and Systems, Chongqing University, Chongqing 400030, China.
Tel.: +86 23 6510 2474; fax: +86 23 6510 2474.
*E-mail address:* zhuxun@cqu.edu.cn (X. Zhu).

0378-7753/$ – see front matter © 2011 Elsevier B.V. All rights reserved.
doi:10.1016/j.jpowsour.2011.04.013

large differences in power generation and structure of microbial community when MFCs were operated at different external resistances. Rismani-Yazdi et al. [22] investigated the effect of external resistance on bacterial diversity and metabolism in MFCs. They found that changes in the external resistance affected not only the power generation, but also the microbial metabolism. Mclean et al. [23] described how difference in external resistances affect cellular electron transfer rates on a per cell basis and overall biofilm development in *Shewanella oneidensis* strain MR-1 by monitoring the real-time microscopic imaging of anode population. They found that the anode of a MFC started up at a low resistance (100 Ω) has a thinner biofilm and higher current per cell, compared with that at a high external resistance (1 MΩ). Moreover, the power production and coulombic efficiency of MFCs can be substantially improved using an automatic control strategy of external resistance as reported by Premier et al. [24].

The external resistance may also influence the MFC performance by affecting the structure of the biofilm in the anode. For an MFC using organic matters as substrate, a lower external resistance usually leads to a higher amount of electrons per unit of time from the biofilm to electrode, and therefore a higher proton production rate in the interior of the biofilm. As a result, when the MFC is operated under a low external resistance, the higher proton production rate will cause a pH drop within the biofilm, which in turn would lead to unfavorable microenvironments for the growth of the electrochemically active bacteria. On the other hand, it is well known that the architecture of the biofilm adapts in response to environmental stresses, such as low nutrient availability, high shear forces, unfavorable pH value and toxic compounds. Therefore, it was reasonable to postulate that the morphology and structure of the biofilm developed at various external resistances would be different dues to the different proton producing rates within the biofilm.

In the present study, four biofilm samples were established in the anode of a two-chamber MFC using acetate as substrate employing anaerobic mixed consortia as anodic inoculums under an external resistance of 10, 50, 250 and 1000 Ω. The objectives of the present study were to assess the effects of external resistance on the start-up process, biofilm formation and structure, as well as the electricity generation of the MFCs.

## 2. Materials and methods

### 2.1. MFC configuration and operation

The experiments were conducted using four two compartment MFCs. Each MFC consisted of a proton exchange membrane (PEM) (Nafion 117, Dupont), two carbon cloth electrodes (E-TEK, B-1A, America) and two plexiglass plates with a flow channel holding a volume of 2.7 mL. The PEM and electrodes had an apparent surface area of 25 $cm^2$. The anode compartment was inoculated with the effluent from a MFC running on acetate. Both anode and cathode compartments were equipped with Ag/AgCl reference electrodes. All MFC tests were conducted in a temperature-controlled room at 25 °C and were repeated three times to check reproducibility of the data.

In order to evaluate the impact of external resistances, the MFCs were started at an external resistance of 10, 50, 250, and 1000 Ω (denoted as MFC-10, MFC-50, MFC-250 and MFC-1000, respectively). After 7 days of operation, fresh anolyte, containing sodium acetate 2.7 g $L^{-1}$, 6 g $L^{-1}$ $Na_2HPO_4$, 3 g $L^{-1}$ $KH_2PO_4$, 0.1 g $L^{-1}$ $NH_4Cl$, 0.5 g $L^{-1}$ NaCl, 0.1 g $L^{-1}$ $MgSO_4{\cdot}7H_2O$, 15 mg $L^{-1}$ $CaCl_2{\cdot}2H_2O$ and 1.0 mL $L^{-1}$ of a trace elements solution, was fed at a rate of 1.5 L $day^{-1}$. To minimize the influence of the cathode potential on the overall cell performance, a 50 mM potassium ferricyanide solution was continuously supplied to the cathode at a rate of 1 mL $min^{-1}$ during the start-up stage and steady-state operation.

### 2.2. Data acquisition and analysis

Cell voltages ($U$), currents ($I$), anode and cathode potentials of each MFC were collected every 15 s via an Agilent 34970A data acquisition unit connected to a PC. In the measurement, the external resistance was varied in a range of $(5–1.0) \times 10^5$ Ω to control the condition of discharging and record the voltage–current curves. After each change in the electrical resistance, the MFCs were held until the current and cell voltage reached steady-state. The power density of the MFCs was calculated according to Eq. (1):

$$P = U \times \frac{I}{A} \tag{1}$$

where $A$ is the surface area of the electrode, $I$ and $U$ are the sustainable current and cell voltage after the MFC reached steady-state, respectively.

The cyclic voltammetry (CV) experiments were carried out in a range from −0.6 to +0.37 V vs. SHE at a scan rate of 5 mV $s^{-1}$ using a Zennium electrochemical workstation (Zahner, Germany) with the anode as the working electrode. The cathode was used as the counter electrode and the reference electrode was an Ag/AgCl reference electrode.

The metabolic energy gain (MEG) for the electrochemically active bacteria was calculated with the following equation described by Wei et al. [19]:

$$MEG = \int_0^t (E_{\text{andoe}}(t) - E^{0'}) I(t)\, dt \tag{2}$$

where $E_{\text{anode}}(t)$ and $I(t)$ are the anode potential and current at time t during start-up period respectively. $E^{0'}$ is the standard potential of $CO_2$/acetate (−0.29 V). The unavailable part of MEG for the electrochemically active bacteria was neglected because this portion make up less than 20% of the MEG when the MFC was started up by applying an external resistance to the electrical circuit [19].

### 2.3. SEM characterization

The morphology of biofilms formed under different external resistances was analyzed by a scanning electron microscopy (SEM) (3400N, HITACHI instrument). At the removal from the anode compartment, the samples was immediately sliced by a sterilized bistoury, and fixed by phosphate buffer saline (PBS) with 2.5% glutaraldehyde (pH 7.2–7.4) for 1 h. The samples were then washed three times with the same buffer and dehydrated stepwise with a graded series of ethanol solutions (30, 50, 70, 80, 90 and 100%). The electrode samples were finally critical-point dried with tert-butyl ethanol and sputter coated with a thin layer of gold. The biofilm was observed in high vacuum using SEM in the secondary electron imaging mode.

### 2.4. Quantization of biofilm components

#### 2.4.1. Biomass quantification by phospholipid method

For the evaluation of total active biomass, small pieces of anode electrode with biofilms were taken from the MFCs and analyzed according to the procedure reported by Verstraete [4] as soon as the current generation was stable. The phosphate concentration released from phospholipids was determined using a Leng Guang 756mc spectrophotometer at 610 nm. Phosphate concentration was then correlated to total active biomass using the conversion factor of 191.7 μg of biomass-C per 100 mmol of phospholipid [25].

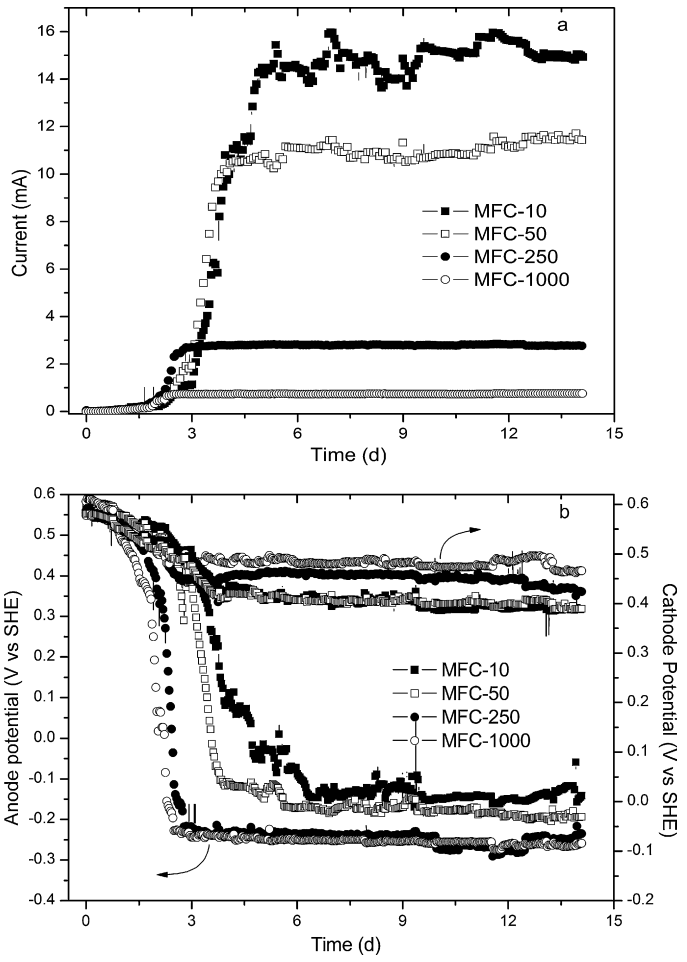


**Fig. 1.** Evolution of current generation (a) and electrode potentials (b) of the MFC started up at various external resistances.

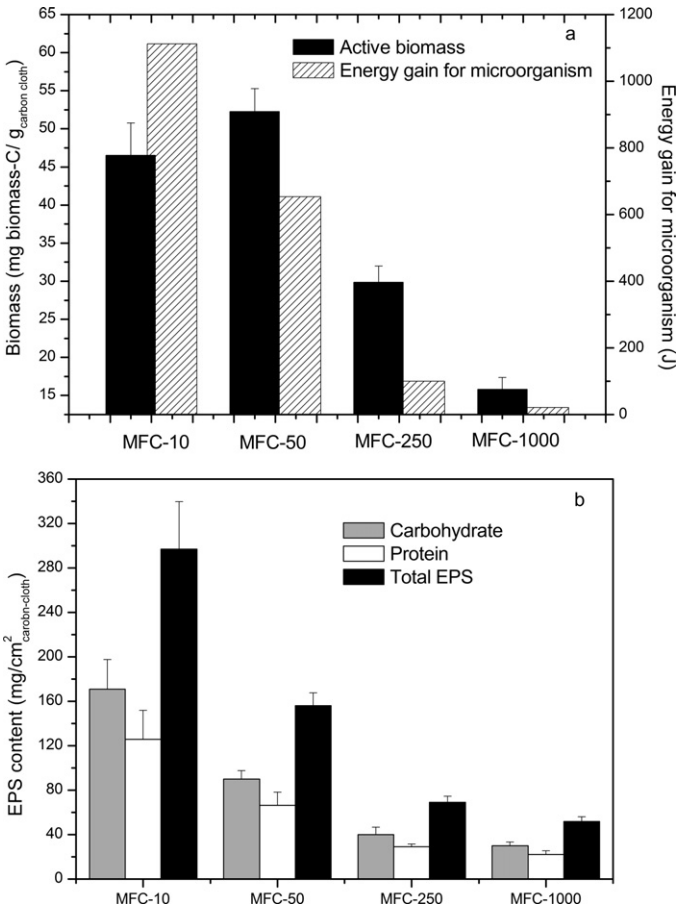


**Fig. 2.** Effect of external resistance on active biomass and energy gain (a) for bacterial growth as well as EPS contents of the biofilms (b) after start-up.

#### 2.4.2. EPS characterization

The characteristics of biofilm EPS (extracellular polymeric substances) in each reactor were analyzed according to Fang et al. [26]. Four biofilm-coated samples were removed from each MFC after the start-up and immersed in 50 mL of a pH 7.5 TE buffer containing 10 mM Trizma base, 10 mM EDTA and 2.5% NaCl. Biofilm was scrapped from each sample, and centrifuged at 3500 rpm for 20 min. The concentrated biomass was then re-suspended in 10 ml of a 0.85% sodium chloride solution containing 0.22% formaldehyde at 80 °C for 30 min for EPS extraction. The EPS dissolved in the formaldehyde solution was recovered by further centrifugation at 3500 rpm for 30 min. The carbohydrate content of EPS ($EPS_c$) in the extracted solution was measured using the phenol/sulfuric-acid method [27] and the protein content ($EPS_p$) using the Lowry method [28]. The sum of $EPS_p$ and $EPS_c$ represented the total EPS of the samples. Lactose and bovine serum albumin were used to make calibration curves for the determination of carbohydrates and proteins EPS, respectively.

## 3. Results and discussion

### 3.1. Influence of external resistance on the start-up process

During the start-up period, the anode compartment was inoculated with the effluent from a MFC running on acetate in a continuous feed mode. As shown in Fig. 1a, both current generation, anode and cathode potential of the MFCs were significantly affected by the external resistance. The lag period for MFC-10 was 2.2 day, reaching 14.6 mA after 6.3 days (Fig. 1). Correspondingly, the potential of the anode and the cathode evolved from their initial potentials to −0.14 V and +0.41 V (vs. SHE), respectively. For MFC-50, a steady state current of about 11.2 mA and anode potential of −0.19 V (vs. SHE) were obtained after a 4.3-day start-up period. Fig. 1 also shows a steady current of 2.8 and 0.7 mA, a steady anode potential of −0.23 and −0.25 V (vs. SHE) and a start-up time of 3.0 and 2.6 days for MFC-250 and MFC-1000, respectively. From these results, it is clear that the MFC with a lower resistance showed a higher steady anode potential and current generation after start-up. During start-up, the power of MFC-10, MFC-50, MFC-250 and MFC-1000 increased from 0 to 1.96, 6.05, 1.95 and 0.64 mW, respectively. Fig. 1 also illustrates that there was no obvious change in current generation and anode potential for the four MFCs after the replacement of fresh anolyte, suggesting successful biofilm establishment on the surface of carbon cloth in the anode chamber.

### 3.2. Influence on active biomass and energy gain for microorganisms

The influence of external resistance on the accumulated active biomass and the energy gain of the biofilms formed at 10, 50, 250 and 1000 Ω during the period of start-up is presented in Fig. 2a. It can be seen that the energy gain for the electrochemically active bacteria decreased with the increase of external resistance from 10 to 1000 Ω. Such a result was expected because a lower external resistance induced a higher current generation and a higher potential difference between the anode potential and the redox potential of acetate, both leading to a higher energy gain for the microorganisms (Eq. (2)). It is also interesting to note that the energy gain for

the electrochemically active bacteria grown at 10 Ω (1112.4 J) was significantly higher than the previously reported range of 0–180 J [19]. This result can be mainly attributed to the higher current densities (6.0 A $m^{-2}$) obtained in this study compared with the previous study (0–2.0 A $m^{-2}$).

From Fig. 2a, it also can be seen that the active biomass of the MFCs increased with the decrease of external resistance from 1000 to 50 Ω, and then decreased with external resistance from 50 to 10 Ω. This trend is inconsistent with previous reports in which a higher biomass production was observed at a lower external resistance because of the increased energy gain for the microorganisms at low resistances [3,12]. This probably related to the fact that a higher portion of energy was consumed for the synthesis of EPS rather than for bacterial growth in the case of MFC-10, as will be shown in the following paragraph.

It is commonly accepted that the energy for microorganism is essential for the maintenance of the bacterial vitality [29]. However, the microorganisms may also produce EPS during growth on the anode surface, consuming energy which is available for bacterial growth [30]. EPS could contribute up to 50–90% of the total organic carbon of biofilms and serves many functions such as promoting the initial attachment of cells to solid surfaces, maturing biofilm structure, and enhancing biofilm resistance to environmental stress and disinfectants. The existence of EPS on the anode surface of bioelectrochemical systems fed with various substrates has been noted in recent studies [31–33]. In this study, the EPS content of the anode biofilms developed at various external resistances after start-up was also estimated and elucidated in Fig. 2b. It appears that the EPS content of biofilm increased as the external resistance increased. For instance, the EPS content of biofilm established during start-up decreased from 296.8 ± 42.9 to 51.9 ± 4.2 mg $g^{-1}_{carbon\text{-}cloth}$ when the external resistance was increased from 10 to 1000 Ω. Considering that the active biomass of the biofilm developed at 10 Ω was lower than that of 50 Ω, whereas the energy gain was higher, this result suggested that a greater portion of energy was consumed for EPS synthesis in the case of the biofilm developed at 10 Ω.

### 3.3. Influence on electrochemical behavior of biofilms

In order to evaluate the importance of mediators produced by the microorganisms for electricity generation, CV tests were conducted on the anode during stable current generation and with depleted substrate. From the voltammograms in Fig. 3, all the biofilms during stable current generation (Fig. 3a) show catalytic behavior for the bioelectrooxidation of acetate by the appearance of an oxidation current at an onset potential of −0.26 V (vs. SHE) during the anodic scan. In the cathodic scan, additional oxidation peaks can be observed around −0.16 V (vs. SHE) and no reduction peaks were found. It is obvious from Fig. 3a that the voltammograms of all the samples exhibited no significant difference, except that the oxidation peak (0.11 V vs. SHE) of the biofilms established at 50 Ω was significantly higher than that obtained from the other samples. This improvement can be attributed to the higher active biomass within the biofilm of MFC-50, as indicated in Fig. 2a. In comparison, all the curves for the anodes with depleted substrate (Fig. 3b) exhibited oxidation peaks at −0.1 V (vs. SHE) and reduction peaks at −0.18 V (vs. SHE). These results are consistent with previous studies [20,34], which were indicative of the existence of mediators produced by the mixed culture. The similarities among these results also suggest that the dominant species in the biofilms were slightly influenced by changes in the external resistance from 10 to 1000 Ω [35]. In addition, considering that the current responses of the anodes during stable current generation were much stronger than that of the redox peaks with depleted substrate, it is reasonable to postulate that direct electron transfer was the main mechanism for current generation by the biofilms.

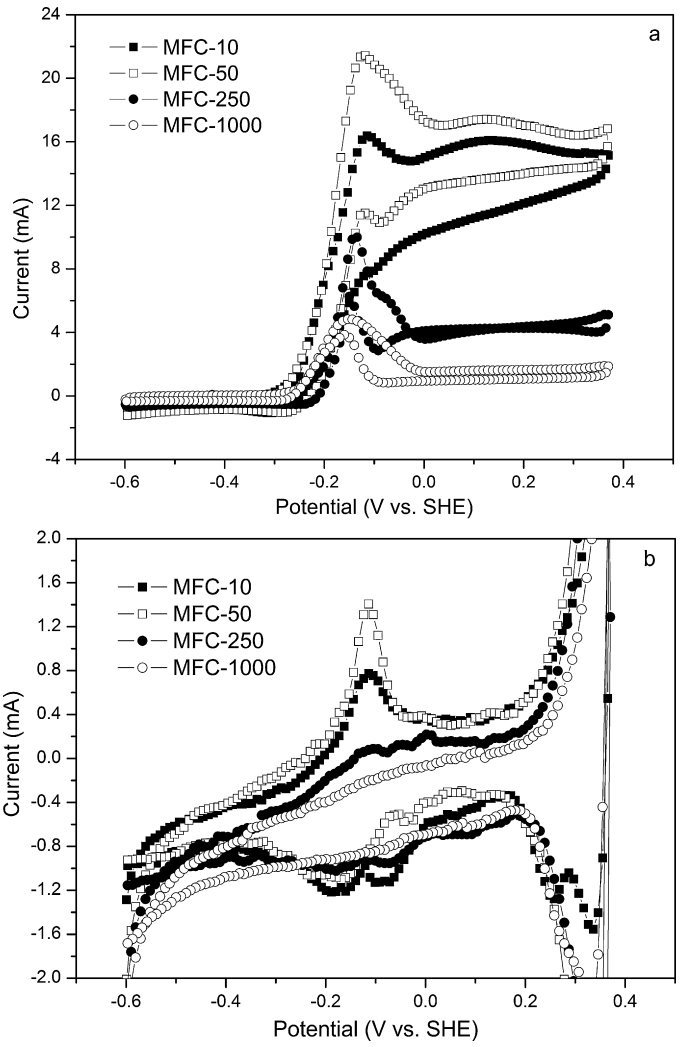


**Fig. 3.** Cyclic voltammograms of the anodes during stable voltage output (a) and with depleted substrate (b).

### 3.4. Influence on biofilm formation

Fig. 4 displays SEM microphotographs of the surface of the anode biofilms grown under different external resistances. Although the morphology of the biofilm may have been altered by the dehydration process, the SEM results provided good comparative information demonstrating clear differences in the architectures of the biofilm established at various external resistances. It can be clearly seen from Fig. 3a–d that the biofilms did not totally cover the electrode surface except for the biofilm developed at 10 Ω. For MFC-10, the entire anode surface was covered by the biofilm, converting the porous, rough electrode surface to a smooth, uniform one. The SEM images at higher magnification (Fig. 4e–h) provide further insight into the morphology of the biofilms formed at different external resistances. Compared with Fig. 4f–h, Fig. 3e indicates that the biofilm established at 10 Ω contained greater amounts of EPS than that of the biofilm developed at 50, 250 and 1000 Ω. This observation corroborates the EPS results seen in Fig. 2b.

The cross sectional morphology of the biofilm samples was also obtained in this study by SEM (Fig. 5). SEM images show that the biofilms were only developed on the surface of the electrode and only few bacteria grew into the porous carbon cloth matrix. This

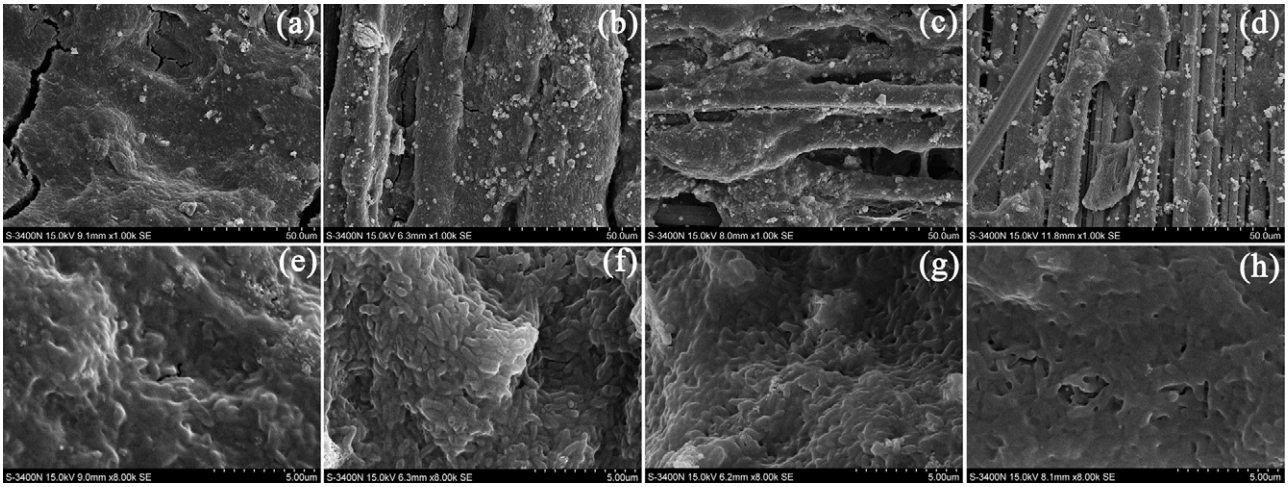


**Fig. 4.** SEM surface micrographs of the biofilm established at 10 Ω (a), 50 Ω (b), 250 Ω (c), 1000 Ω (d) and higher magnification of a (e), b (f), c (g), d (h).

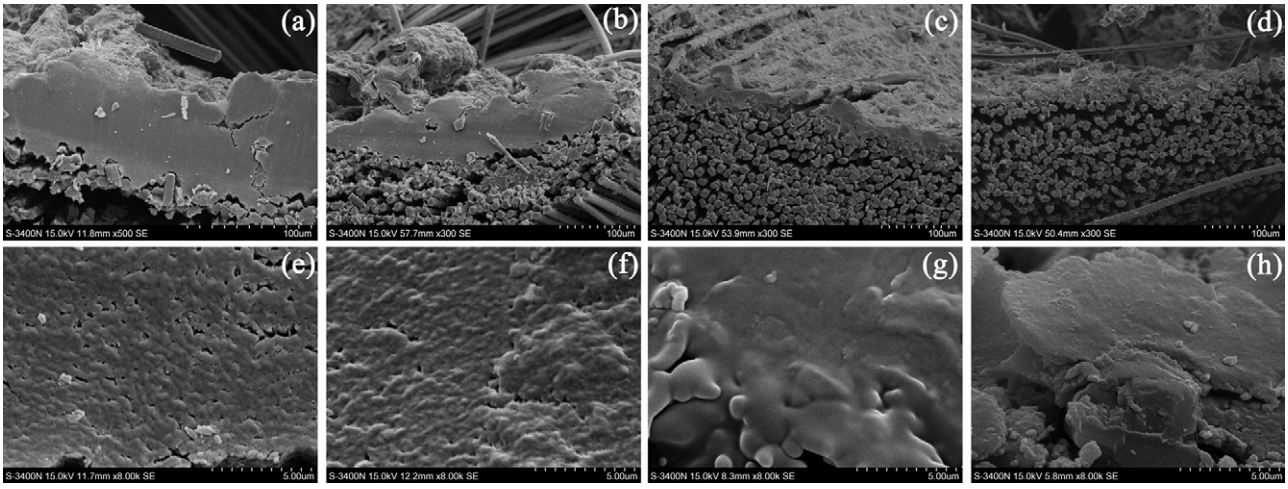


**Fig. 5.** SEM cross-sectional images of the biofilm established at 10 Ω (a), 50 Ω (b), 250 Ω (c), 1000 Ω (d) and higher magnification of a (e), b (f), c (g), d (h).

could be attributed to both the small pore size and the limited substrate supply within the carbon cloth matrix. Similar phenomenon was also observed when reticulated vitreous carbon was used as anode support [31]. In addition, as can be seen in Fig. 5, all the biofilms exhibited substantial heterogeneity in thickness. The average thicknesses of the biofilms formed under 10 (Fig. 5a) and 50 Ω (Fig. 5b) was significantly higher than that at 250 (Fig. 5c) and 1000 Ω (Fig. 5d). This result can be mainly attributed to the higher active biomass and EPS content in the biofilm samples established at 10 and 50 Ω. It is also interesting to note that although the biofilm formed at 10 Ω contained less active biomass than that at 50 Ω, both biofilms were of similar thickness. Putting these results together and recalling that the biofilm formed at 10 Ω contained more EPS than that at 50 Ω, one could assumed that the bacteria was more loosely packed in the biofilm developed at 10 Ω. In order to further confirm this point, the microstructures of the biofilms formed at different external resistances were observed in higher magnification (Fig. 5e–h). It can be clearly seen from these figures that the extensive voids were found to be distributed within biofilm established at 10 Ω. These voids were beneficial for mass transport within the biofilm by forming water channels that facilitate the substrate and buffer supply, as well as product removal. It should be pointed out, however, that the existence of void spaces within the biofilms would also lead to imperfect contact between the electroactive microorganisms and the anodes, causing a decrease in the electrical conductivity of the biofilm matrixes and consequently the lowered performance of the MFCs. By contrast, the biofilm formed at 50, 250 and 1000 Ω (Fig. 5f–h) appeared quite homogeneous throughout its thickness and few voids can be discerned. Based on the results from the surface and cross-sectional SEM images, it is apparent that the biofilms developed at 50, 250 and 1000 Ω showed a compact structure, in which cells are tightly linked together by visible polymeric viscous materials.

### 3.5. Influence on electricity generation

Fig. 6 compared the polarization curves of the MFCs (10 kΩ to 5 Ω) started up at different external resistances. The details of the MFC performance were summarized in Table 1. As illustrated in Fig. 6 and Table 1, the maximum power density of the MFCs decreased in the following order: MFC-50 > MFC-250 > MFC-10 > MFC-1000. The best performance of MFC-50 may come from the highest active biomass production (Fig. 2a) on the surface of the carbon paper. The lower performance of MFC-10, despite the higher active biomass, might be due to the significant ohmic loss (Table 1) resulting from the existence of void spaces in the interior of the biofilm.

More importantly, it is clear from Fig. 6b that there were steep falls of cell voltage at relatively high current densities in the case of MFC-50, MFC-250 and MFC-1000, whereas a gradually decrease in

**Table 1**
Details of the performance of the MFCs started up at various external resistances.

| MFC sample | $P_{max}$ (W m$^{-2}$) | $I_{max}$[a] (A m$^{-2}$) | Open circuit voltage (V) | Internal resistance (Ω) |
|---|---|---|---|---|
| MFC-10 | 1.25 ± 0.01 | 8.49 ± 0.19 | 0.817 | 28.1 ± 2.1 |
| MFC-50 | 2.61 ± 0.18 | 5.78 ± 0.39 | 0.821 | 3.8 ± 1.5 |
| MFC-250 | 1.53 ± 0.01 | 2.46 ± 0.02 | 0.820 | 9.5 ± 3.2 |
| MFC-1000 | 0.93 ± 0.02 | 1.25 ± 0.01 | 0.824 | 13.9 ± 3.1 |

[a] Maximum sustainable current density.

the cell voltage with the increase of current density can be noted for MFC-10. The experiments were repeated three times with similar results. The rapid fall of cell voltage at high current densities is a common phenomenon for both single [36–38] and stacked MFCs [39]. In order to further study this phenomenon, the variation of the voltage of the MFCs with step-change of external resistance during performance evaluation were recorded and shown in Fig. 7. As can be seen in Fig. 7, a slow decrease of voltage with time followed by a steep fall of voltage output was observed when an external resistance of 150, 50 and 20 Ω was connected to the electrical circuit of MFC-1000, MFC-250 and MFC-50, respectively. Whereas in the case of MFC-10, a stable voltage was reached within 20 min even when the external resistance as low as 5 Ω was applied. As a consequence, MFC-10 exhibits a highest maximum sustainable current density ($I_{max}$) of 8.49 ± 0.19 A m$^{-2}$ (Table 1), while MFC-50, MFC-250 and MFC-1000 reached a limit of 5.78 ± 0.39, 2.46 ± 0.02 and 1.25 ± 0.01 A m$^{-2}$, respectively. The observed differences can be explained by the improved buffer access and proton removal in the case of the biofilm developed at 10 Ω.

It is well known that the electrochemical oxidation of acetate is an acid-producing process. In the anode compartment, acetate is oxidized according to the following reaction:

$$CH_3COO^- + 2H_2O \rightarrow 2CO_2 + 7H^+ + 8e^-$$

As shown in the above equation, the oxidation of every mole of acetate produces 7 mol of proton, which can result in a pH decrease within the biofilm microenvironment. This can lead to an increase in the potential for acetate oxidation and an inhabitation of microbial metabolism, both negatively influencing the MFC performance [40]. When a MFC was operated at a high current density or a low resistance, this problem becomes more serious due to the higher proton production rate. For MFC-50, MFC-250 and MFC-1000, the compact structure of the biofilms (Fig. 5f–h) hindered the buffer

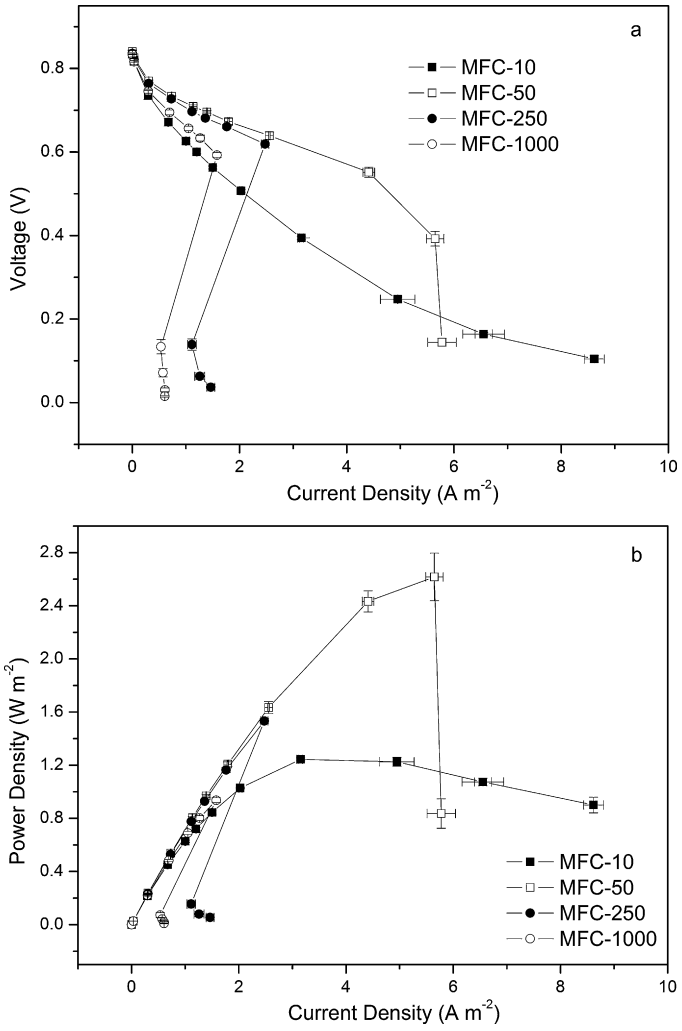


**Fig. 6.** Effect of external resistance on (a) polarization and (b) power–current properties of the MFCs started up at different external resistances.

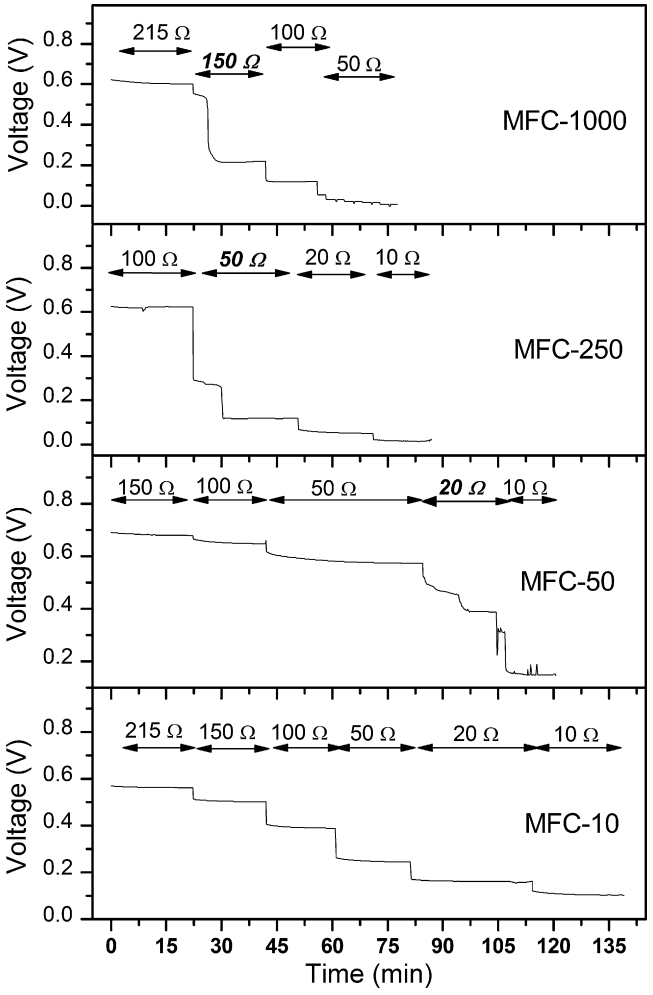


**Fig. 7.** Variation of the voltage of the MFCs with step-change of external resistance during the performance evaluation.

access and proton removal, leading to gradual accumulation of proton in the interior of the biofilm. When the proton concentration within the biofilm exceeded a critical value, the current generation of the MFCs became unsustainable over time due to the inhibition of the electrochemically active bacteria. Correspondingly, steep drops in cell voltage were observed (Fig. 7a–c). By contract, the biofilm formed at 10 Ω has a looser structure (Fig. 5e) with void spaces within the biofilm. These characteristics facilitated water and buffer access as well as proton removal. As a result, the highest sustainable current can be obtained by MFC-10 due to the maintenance of the favorable microenvironment for the microorganisms within the anode biofilm.

## 4. Conclusions

In the present study, the effects of external resistance on the biofilm formation and electricity generation were investigated. Structural and morphological characterizations of the biofilms formed at various external resistances indicate that a suitable biofilm structure is crucial for the maximum power density and sustainable current generation of the MFCs. The experimental results showed that the biofilm established at a higher external resistance tended to form a compact structure with a less active biomass and a lower EPS content. This led to an increase of the maximum power density with the decrease of external resistance. However, when the external resistance became lower than the optimum value, a loose biofilm structure with a less active biomass and a higher EPS content was developed, resulting in more void spaces beneficial for proton and buffer transport and reduction of the electrical conductivity within the biofilm. Therefore, a lower maximum power density and higher maximum sustainable current generation can be obtained.

## Acknowledgements

This work was supported by the National Natural and Science Foundation of China (Nos. 50806087 and 50825602), and Fundamental Research Funds for the Central Universities (No. CDJXS11142230). The authors also wish to thank Ms. Lu at the Central laboratory of Third Military Medical University for assistance in SEM measurements.

## References

[1] B.E. Logan, B. Hamelers, R. Rozendal, U. Schröder, J. Keller, S. Freguia, P. Aelterman, W. Verstraete, K. Rabaey, Environ. Sci. Technol. 40 (2006) 5181–5192.
[2] K. Rabaey, W. Verstraete, Trends Biotechnol. 23 (2005) 291–298.
[3] S. Freguia, K. Rabaey, Z. Yuan, J. Keller, Environ. Sci. Technol. 41 (2007) 2915–2921.
[4] P. Aelterman, S. Freguia, J. Keller, W. Verstraete, K. Rabaey, Appl. Microbiol. Biotechnol. 78 (2008) 409–418.
[5] X. Cao, X. Huang, N. Boon, P. Liang, M. Fan, Electrochem. Commun. 10 (2008) 1392–1395.
[6] H. Liu, R. Ramnarayanan, B.E. Logan, Environ. Sci. Technol. 38 (2004) 2281–2285.
[7] S. You, Q. Zhao, J. Zhang, J. Jiang, C. Wan, M. Du, S. Zhao, J. Power Sources 173 (2007) 172–177.
[8] Q. Deng, X. Li, J. Zuo, A. Ling, B.E. Logan, J. Power Sources 195 (2010) 1130–1135.
[9] Y. Feng, Q. Yang, X. Wang, B.E. Logan, J. Power Sources 175 (2010) 1841–1844.
[10] H. Liu, S. Cheng, L. Huang, B.E. Logan, J. Power Sources 179 (2008) 274–279.
[11] U. Schröder, J. Nießen, F. Scholz, Angew. Chem. Int. Ed. 115 (2003) 2986–2989.
[12] P. Aelterman, M. Versichele, M. Marzorati, N. Boon, W. Verstraete, Bioresour. Technol. 99 (2008) 8895–8902.
[13] G.C. Gil, I.S. Chang, B.H. Kim, M. Kim, J.K. Jang, H.S. Park, H.J. Kim, Biosens. Bioelectron. 18 (2003) 327–334.
[14] G.S. Jadhav, M.M. Ghangrekar, Bioresour. Technol. 100 (2009) 717–723.
[15] T. Catal, P. Kavanagh, V. O'Flaherty, D. Leech, J. Power Sources 196 (2011) 2676–2681.
[16] R.C. Wagner, D.F. Call, B.E. Logan, Environ. Sci. Technol. 44 (2010) 6036–6041.
[17] D.A. Finkelstein, L.M. Tender, J.G. Zeikus, Environ. Sci. Technol. 40 (2006) 6990–6995.
[18] X. Wang, Y. Feng, N. Ren, H. Wang, H. Lee, N. Li, Q. Zhao, Electrochim. Acta 54 (2009) 1109–1114.
[19] J. Wei, P. Liang, X. Cao, X. Huang, Environ. Sci. Technol. 44 (2010) 3187–3191.
[20] H. Liu, S. Cheng, B.E. Logan, Environ. Sci. Technol. 39 (2005) 658–662.
[21] D.Y. Lyon, F. Buret, T.M. Vogel, J.M. Monier, Bioelectrochemistry 78 (2010) 2–7.
[22] H.R. Rismani-Yazdi, A.D. Christy, S.M. Carver, Z. Yu, B.A. Dehority, O.H. Tuovinen, Bioresour. Technol. 102 (2011) 278–283.
[23] J.S. Mclean, G. Wanger, Y.A. Gorby, M. Wainstein, J. Mcquaid, S.I. Ishii, O. Bretschger, H. Beyenal, K.H. Nealson, Environ. Sci. Technol. 44 (2010) 2721–2727.
[24] G.C. Premier, J.R. Kim, I. Michie, R.M. Dinsdale, A.J. Guwy, J. Power Sources 196 (2011) 2013–2019.
[25] R.H. Findlay, G.M. King, L. Watling, Appl. Environ. Microbiol. 55 (1989) 2888–2893.
[26] H.H.P. Fang, L.C. Xu, K.Y. Chan, Water Res. 36 (2002) 4709–4716.
[27] A.F. Gaudy, Ind. Water Wastes 7 (1962) 17–22.
[28] O.H. Lowry, N.J. Rosebrough, A.L. Farr, R.J. Randall, J. Biol. Chem. 193 (1951) 265–275.
[29] U. Schröder, Phys. Chem. Chem. Phys. 9 (2007) 2619–2629.
[30] N. Qureshi, B.A. Annous, T.C. Ezeji, P. Karcher, I.S. Maddox, Cell. Fact 4 (2005) 24–44.
[31] C.I. Torrres, R. Krajmalnik-brown, P. Parameswaran, A. Kato Marcus, G. Wanger, Y.A. Gorrby, B.E. Rittmann, Environ. Sci. Technol. 43 (2009) 9519–9524.
[32] H. Yi, K.P. Nevin, B.C. Kim, A.E. Franks, A. Klimes, L.M. Tender, D.R. Lovely, Biosens. Bioelectron. 24 (2009) 3498–3503.
[33] A. Larrosa-Guerrero, K. Scott, K.P. Katuri, C. Godinez, I.M. Head, T. Curtis, Appl. Microbiol. Biotechnol. 87 (2010) 1669–1713.
[34] J.R. Kim, S.H. Jung, J.M. Regan, B.E. Logan, Bioresour. Technol. 98 (2007) 2568–2577.
[35] S.A. Patil, F. Harnisch, B. Kapadnis, U. Schröder, Biosens. Bioelectron. 26 (2010) 803–808.
[36] B. Min, Ó.B. Román, I. Angelidaki, Biotechnol. Lett. 30 (2008) 1213–1218.
[37] D.P.B.T.B. Strik, H. Terlouw, H.V.M. Hamelers, C.J.N. Buisman, Appl. Microbiol. Biotechnol. 81 (2008) 659–668.
[38] A. Heijne, H.V.M. Hamelers, M. Saakes, C.J.N. Buisman, Electrochim. Acta 53 (2008) 5697–5703.
[39] P. Aelterman, K. Rabaey, H.T. Pham, N. Boon, W. Verstraete, Environ. Sci. Technol. 40 (2006) 3388–3394.
[40] C.I. Torres, A.K. Marcus, B.E. Rittmann, Biotechnol. Bioeng. 100 (2008) 872–881.